Spectroscopic determination of hole density in the ferromagnetic semiconductor $Ga_{1-x}Mn_xAs$

M. J. Seong,[1,*] S. H. Chun,[2] H. M. Cheong,[1,3] N. Samarth,[2] and A. Mascarenhas[1]
[1]*National Renewable Energy Laboratory, 1617 Cole Boulevard, Golden, Colorado 80401*
[2]*Department of Physics and Materials Research Institute, The Pennsylvania State University, University Park, Pennsylvania 16802*
[3]*Department of Physics, Sogang University, Seoul 121-742, Korea*
(Received 8 May 2002; published 3 July 2002)

A measurement of the hole density in the ferromagnetic semiconductor $Ga_{1-x}Mn_xAs$ is notoriously difficult using standard transport techniques due to the dominance of the anomalous Hall effect. Here we report a spectroscopic measurement of the hole density in four $Ga_{1-x}Mn_xAs$ samples ($x=0$, 0.038, 0.061, and 0.083) at room temperature using a Raman-scattering intensity analysis of the coupled plasmon–LO-phonon mode and the unscreened LO phonon. The unscreened LO-phonon frequency linearly decreases as the Mn concentration increases up to 8.3%. The hole density determined from the Raman scattering shows a monotonic increase with increasing x for $x \leqslant 0.083$, exhibiting a direct correlation to the observed T_c. The optical technique reported here provides an unambiguous means of determining the hole density in this important class of ''spintronic'' semiconductor materials.

DOI: 10.1103/PhysRevB.66.033202 PACS number(s): 75.50.Pp, 78.30.Fs

Current interest in the development of a semiconductor ''spintronics'' technology[1] provides a strong motivation for fundamental studies of diluted magnetic semiconductors (DMS's).[2–4] These are semiconductors that incorporate magnetic ions such as Mn^{2+} within the crystal lattice. Paramagnetic (and antiferromagnetic) DMS's have traditionally been realized by incorporating isovalent transition-metal ions into II-VI semiconductors such as CdTe and ZnSe.[2,3] The relatively recent discovery of III-V semiconductor-based ferromagnetic DMS's with Curie temperatures (T_c) as high as 110 K has now raised interesting fundamental issues regarding the origin of ferromagnetism in materials such as $Ga_{1-x}Mn_xAs$.[5–7] In these III-V DMS's, Mn^{2+} acts as an acceptor, generating free holes in the valence band.[8] The ferromagnetism in these materials arises from the exchange interaction between these holes and the Mn^{2+} ions, and it is generally believed that there is a direct correlation between T_c and the hole density p.[5,9] However, the unambiguous determination of the hole density in $Ga_{1-x}Mn_xAs$ by standard magnetotransport techniques (Hall measurement) is difficult because of the anomalous Hall effect. The extraction of the ordinary Hall effect from the measurement, applied at $T \ll T_c$, requires magnetic fields larger than 20 T even at temperatures as low as 50 mK; even under these conditions, the measured Hall data are not completely free from the effect of the negative magnetoresistance, resulting in significant uncertainty in the deduced hole density. In addition, Hall measurements are not applicable to magnetically dilute samples that are insulating.[4] Finally, we note that the Curie-Weiss law behavior of the magnetic susceptibility *determined by the Hall effect* clearly indicates the dominance of the anomalous Hall effect over the ordinary Hall effect even at room temperature.[10] Here we exploit an alternative method (Raman scattering) to determine the hole density in $Ga_{1-x}Mn_xAs$ epilayers for a wide range of temperatures by correlating the hole density to the coupled plasmon–LO-phonon mode (CPLOM).[11,12] Our results show that this spectroscopic technique provides a reliable method for determining the hole density in ferromagnetic semiconductors over a broad range of sample conductivity, ranging from insulating to highly metallic.

For *n*-type GaAs, the coupling between the LO phonon and electron plasmon results in two Raman-active coupled plasmon–LO-phonon modes L^+ and L^-. For a high electron density, L^+ shows a rapid blueshift with increasing electron concentration, providing an accurate calibration for the electron concentration, whereas L^- remains almost stationary near the GaAs TO frequency. On the other hand, only one CPLOM is observed in *p*-type GaAs due to a strong hole plasmon damping, moving from the LO frequency to the TO frequency with increasing hole concentration.[12] In this paper, we report on a spectroscopic determination of the carrier concentration of four $Ga_{1-x}Mn_xAs$ samples ($x=0$, 0.038, 0.061, and 0.083) at room temperature using Raman scattering from CPLOM. We find that the unscreened LO (ULO) phonon frequency of $Ga_{1-x}Mn_xAs$ decreases significantly as the Mn concentration increases up to 8.3%. This makes the traditional lineshape analysis for a typical *p*-type GaAs, where the doping does not change the ULO frequency, unsuitable for determining the hole density in $Ga_{1-x}Mn_xAs$. By analyzing the relative Raman intensities of the ULO phonon and the CPLOM, however, we were able to determine the carrier concentration up to 7×10^{20} cm^{-3}. The monotonic increase of the hole density with increasing x for $x \leqslant 0.083$ correlates well with the change of T_c.

$Ga_{1-x}Mn_xAs$ epilayers with a thickness of $\sim$120 nm were grown by molecular-beam epitaxy at $\sim$250 °C on a (001) semi-insulating GaAs substrate after the deposition of a buffer structure consisting of a 120-nm standard GaAs epilayer grown at $\sim$550 °C followed by a 60-nm low-temperature-grown GaAs epilayer. Electron microprobe analysis (EMPA) was used to determine Mn concentrations. Details about the growth conditions and parameters are described elsewhere.[13] Raman-scattering measurements were

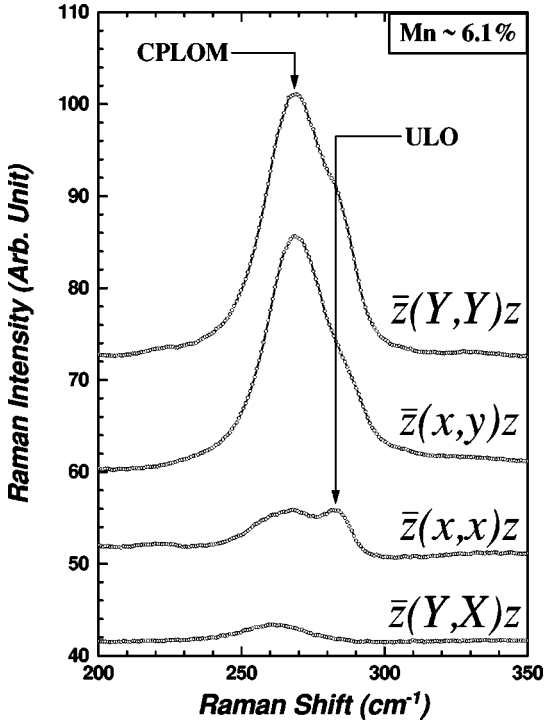

FIG. 1. Raman spectra of $Ga_{1-x}Mn_xAs$ with 6.1% Mn at room temperature for 457-nm excitation in a quasibackscattering geometry with different polarization configurations, where $z=[001]$, $x=[100]$, $Y=[110]$, etc. The base lines are vertically shifted for clarity.

performed at room temperature in a quasibackscattering geometry on the (001) growth surface of the samples. The 457-nm line from a Coherent Ar^+ laser was used as an excitation light source in order to obtain a very short penetration depth, thus avoiding any Raman scattering from the buffer layers. The scattered photons were dispersed by a SPEX 0.6-m triple spectrometer and detected with a liquid-nitrogen-cooled charge-coupled-device detector. The spectrometer was calibrated using the frequency of the longitudinal optical phonon peak (292 cm^{-1}) of a separate GaAs reference sample.

Typical Raman spectra of $Ga_{1-x}Mn_xAs$ with 6.1% Mn at room temperature in a quasibackscattering geometry with different polarization configurations are displayed in Fig. 1, where $z=[001]$ is the growth direction and $x=[100]$, $y=[010]$, $X=[1\bar{1}0]$, and $Y=[110]$. According to the Raman selection rule for a zinc-blende crystal, the LO phonon is allowed for $\overline{z}(Y,Y)z$ and $\overline{z}(x,y)z$ but forbidden for $\overline{z}(x,x)z$ and $\overline{z}(Y,X)z$, whereas the TO phonon is forbidden for all the scattering configurations employed in Fig. 1.[14] The Raman feature near 269 cm^{-1} is very strong in $\overline{z}(Y,Y)z$ and $\overline{z}(x,y)z$, whereas it is extremely weak in $\overline{z}(Y,X)z$ and $\overline{z}(x,x)z$ where LO modes are forbidden. This reveals its "LO mode" nature despite its proximity to the GaAs TO frequency. The very weak Raman signal near $\sim$266 cm^{-1} in $\overline{z}(Y,X)z$ configuration is the disorder-induced TO phonon that should exist as a weak background Raman intensity for all the other scattering configurations employed in Fig. 1.

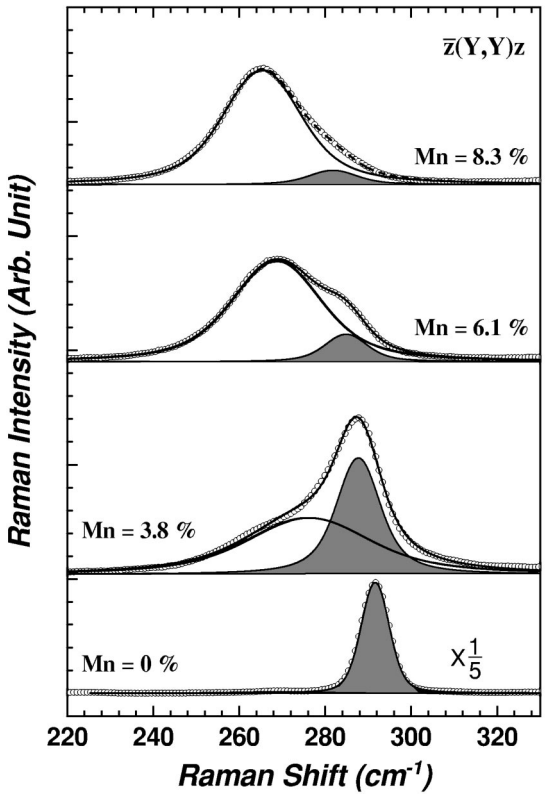

FIG. 2. Raman spectra of $Ga_{1-x}Mn_xAs$ for $x=0$, 0.038, 0.061, and 0.083 at room temperature for 457-nm excitation in a $\overline{z}(Y,Y)z$ scattering configuration, where open circles represent experimental data. The shaded area corresponds to the unscreened LO-phonon component, and the solid curves represent contributions from plasmon LO-phonon coupled mode. The base lines are vertically shifted for clarity, and the Raman intensity of the reference sample was scaled down by 1/5.

Thus the Raman feature at 269 cm^{-1} is a CPLOM in $Ga_{0.94}Mn_{0.06}As$. We have not observed any Raman signature in the high frequency spectral range up to 1700 cm^{-1} that can be attributed to L^+. This indicates that the free carrier is a hole. Apart from the strong CPLOM in $\overline{z}(Y,Y)z$, there is an unmistakable shoulder on the high-frequency side of the CPLOM. This is due to the ULO in the depletion layer near the surface. It is more distinctly observed in $\overline{z}(x,x)z$, where the LO mode is forbidden due to Raman selection rules. However, the electric field near the semiconductor surface causes a relaxation of Raman selection rules.

In the $\overline{z}(Y,Y)z$ configuration, the superimposed Raman features can be decomposed into CPLOM and ULO parts by fitting the experimental data using two Lorentzian oscillators as shown in Fig. 2, where Raman spectra of $Ga_{1-x}Mn_xAs$ for $x=0$, 0.038, 0.061, and 0.083 in a $\overline{z}(Y,Y)z$ scattering configuration are displayed. It should be noted that the Raman spectrum of the reference sample ($x=0$) consists of only one Lorentzian oscillator. The Raman intensity of the ULO (shaded area) rapidly decreases as the Mn concentration increases. The peak positions of the CPLOM and ULO determined from the curve fitting are listed in Table I and shown in Fig. 3. The ULO frequency linearly decreases with

TABLE I. Peak positions of the coupled plasmon–LO-phonon mode (CPLOM) and unscreened LO (ULO) determined from Raman scattering. The depletion layer thickness d and the hole concentration p are calculated using Eqs. (3) and (5) with $\xi_S \simeq 2$ and $\phi_B = 0.5$ V.

Mn concentration (%)	ULO (cm^{-1})	CPLOM (cm^{-1})	d (Å)	p (cm^{-3})
0	291.7±1.0			
3.8±0.2	287.7±1.0	276.4±1.0	76±4	$1.2\pm0.2\times10^{19}$
6.1±0.2	284.8±1.0	268.7±1.0	16±1	$2.8\pm0.4\times10^{20}$
8.3±0.2	281.8±1.0	265.3±1.0	10±0.5	$7.1\pm0.7\times10^{20}$

increasing Mn concentrations up to 8.3%. Since the lattice constant of $Ga_{1-x}Mn_xAs$ increases with increasing x the compressive strain in the GaMnAs layer should induce a blueshift of the ULO frequency. However, the alloying effect appears to be much stronger than the strain effect in $Ga_{1-x}Mn_xAs$, leading to the observed ULO frequency redshift with increasing x.

Traditionally, a line-shape analysis of Raman scattering for the CPLOM has been used to deduce carrier concentrations of p-type GaAs,[12,15] assuming that the phonon frequencies of the TO and LO phonon do not change with doping. This is valid because conventional dopant concentrations are too small to change most of the physical parameters of GaAs used for the line-shape analysis. However, Mn concentrations in $Ga_{1-x}Mn_xAs$ samples for $p > 10^{18}$ cm^{-3} are high enough to change the frequency of the ULO as shown in Table I, making it incorrect to use the GaAs parameters for the line-shape analysis of the CPLOM. Alternatively the p-type carrier concentration can be determined by analyzing the relative intensities of ULO and CPLOM.[12] Assuming the Raman-scattering efficiency from the ULO is similar to that in an undoped crystal, the integrated intensity A_L of the ULO can be written as[16]

$$A_L = A_0[1 - \exp(-2\alpha d)], \tag{1}$$

where A_0 is the integrated intensity in an undoped crystal, α is the absorption coefficient, and d is the depletion layer thickness. Since the integrated Raman intensity is proportional to the scattering volume, A_0 is given by

$$A_0 = \xi_S A_P + A_L, \tag{2}$$

where A_P is the integrated intensity of the CPLOM and $\xi_S = I_L/I_P$ is the relative Raman scattering efficiencies of the ULO and CPLOM in a unit volume. Using Eqs. (1) and (2), d can be estimated from the experimental Raman data,

$$d = \frac{1}{2\alpha}\ln\left(1 + \frac{\xi_A}{\xi_S}\right), \tag{3}$$

where $\xi_A = A_L/A_P$ is the ratio of the integrated intensity of the ULO to that of the CPLOM in the Raman spectrum. The depletion layer thickness d for $p > 10^{18}$ can be calculated as a function of hole concentration p at zero temperature (neglecting the transition region),

$$d = \left(\frac{2\varepsilon_0\varepsilon_S\phi_B}{e}\right)^{1/2}\frac{1}{p^{1/2}}, \tag{4}$$

where ε_S is the static dielectric constant and ϕ_B is the surface potential barrier.[12] Since the values of ε_S and ϕ_B for $Ga_{1-x}Mn_xAs$ are not available we used those for GaAs, $\varepsilon_S = 12.8$ (Ref. 17) and $\phi_B = 0.5 \pm 0.05$ V (Ref. 18). By comparing I_L for $x = 0$ and I_P for $x = 0.082$ in Fig. 2 we have obtained $\xi_S \simeq 2$ and used this value for the analysis of all x. Since the ULO Raman efficiency in principle could be dependent on x there is a small uncertainty introduced by using a constant value of $\xi_S \simeq 2$. But a close inspection showed that $A_0 = (2A_P + A_L)$ is almost constant for all four samples, making $\xi_S = 2 \pm 0.1$ a good approximation. We also used $\alpha \simeq 2.0\times10^5$ cm^{-1} for the excitation wavelength 457 nm.[19] By equating Eqs. (4) and (3), p is given by

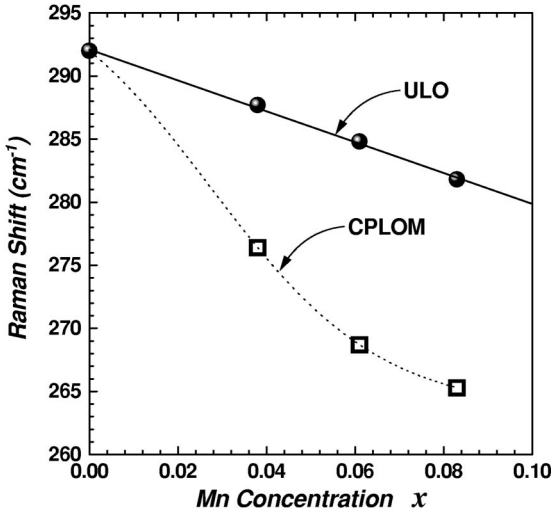

FIG. 3. Mn composition dependence of the LO-phonon (full circle) Raman frequency in $Ga_{1-x}Mn_xAs$ ($x \leqslant 0.083$), where the solid line is a linear fit. CPLOM frequencies are also displayed with a dashed line to guide the eye.

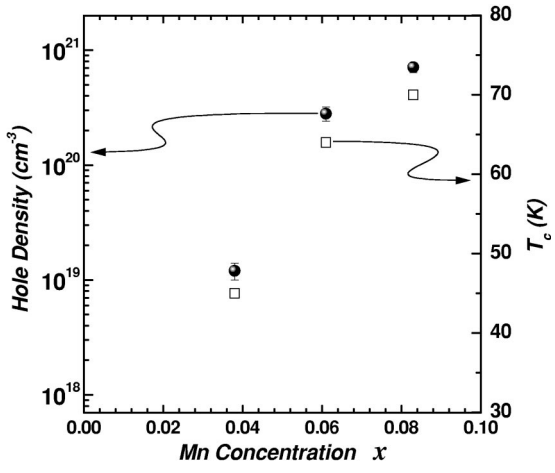

FIG. 4. Mn composition dependence of the hole density determined by Raman scattering (full circles) and the ferromagnetic transition temperature (open squares) for the same set of $Ga_{1-x}Mn_xAs$ samples.

$$p = \frac{8\varepsilon_0\varepsilon_S\alpha^2\phi_B}{e\left[\ln\left(1+\frac{\xi_A}{\xi_S}\right)\right]^2}, \tag{5}$$

and thus calculated hole concentrations are listed in Table I, with an uncertainty less than 10%. It is worth mentioning here that any possible uncertainty in ϕ_B and ε_S would affect only the scaling factor in Eq. (5). In order to check any possible finite-temperature correction in our analysis, we have analyzed the Raman spectrum of the 6.1% sample measured at $T=8$ K and obtained the same hole concentration within the error bar as shown in Table I. The hole concentration monotonically increases up to 7×10^{20} for the 8.3% sample, showing a good correlation with T_c (Fig. 4). This is different from the results of Matsukura *et al.*,[8] where the hole concentration, measured using the Hall effect, and T_c reached their maximum values 1.5×10^{20} cm^{-3} and 110 K, respectively, for $x=0.053$ and then decreased with increasing Mn concentration for $x>0.053$. The difference between the two results can be attributed to differences in detailed growth conditions. However, the fact that the hole concentration, determined by Raman scattering, and T_c show similar monotonic increases with increasing x provides further confidence in our spectroscopically determined values of the hole density in $Ga_{1-x}Mn_xAs$.

In conclusion, we have determined the room-temperature carrier concentration in $Ga_{1-x}Mn_xAs$ for $x=0.038$, 0.061, and 0.083 using a Raman intensity analysis of the coupled plasmon–LO-phonon mode and the unscreened LO phonon. This study shows that—unlike standard Hall measurements—Raman scattering provides an unambiguous and reliable method of determining the hole density in $Ga_{1-x}Mn_xAs$ that can be profitably exploited for gaining a better understanding of the origins of ferromagnetism in ferromagnetic semiconductors.

Work at NREL was supported by the Office of Science (Material Science Division) of the Department of Energy under Contract No. DE-AC36-99GO10337 as well as the NREL DDRD program. Work at PSU was supported by DARPA and ONR under Grant Nos. N00014-99-1-1093, N00014-99-1-0071, and N00014-99-1-0716. H.M.C. was supported by Grant No. 2000-2-30100-009-3 from the Basic Research Program of the Korea Science and Engineering Foundation.

*Corresponding author. Email address: mseong@nrel.gov

[1] S. A. Wolf, D. D. Awschalom, R. A. Buhrman, J. M. Daughton, S. von Molnar, M. L. Roukes, A. Y. Chtchelkanova, and D. M. Treger, Science **294**, 1488 (2001).

[2] *Diluted Magnetic Semiconductors*, edited by J. K. Furdyna and J. Kossut, Semiconductors and Semimetals Vol. 25 (Academic, New York, 1988).

[3] D. D. Awschalom and N. Samarth, J. Magn. Magn. Mater. **200**, 130 (1999), and references therein.

[4] H. Ohno and J. Magn. Magn. Mater. **200**, 110 (1999), and references therein.

[5] T. Dietl, H. Ohno, F. Matsukura, J. Cibert, and D. Ferrand, Science **287**, 1019 (2000).

[6] H. Ohno, A. Shen, F. Matsukura, A. Oiwa, A. Endo, S. Katsumoto, and Y. Iye, Appl. Phys. Lett. **69**, 363 (1996).

[7] J. De Boeck, R. Oesterholt, A. Van Esch, H. Bender, C. Bruynseraede, C. Van Hoof, and G. Borghs, Appl. Phys. Lett. **68**, 2744 (1996).

[8] F. Matsukura, H. Ohno, A. Shen, and Y. Sugawara, Phys. Rev. B **57**, R2037 (1998).

[9] J. König, H. H. Lin, and A. H. MacDonald, Phys. Rev. Lett. **84**, 5628 (2000).

[10] H. Ohno and F. Matsukura, Solid State Commun. **117**, 179 (2001).

[11] A. Mooradian and G. B. Wright, Phys. Rev. Lett. **16**, 999 (1966).

[12] G. Irmer, M. Wenzel, and J. Monecke, Phys. Rev. B **56**, 9524 (1997).

[13] S. J. Potashnik, K. C. Ku, S. H. Chun, J. J. Berry, N. Samarth, and P. Schiffer, Appl. Phys. Lett. **79**, 1495 (2001).

[14] We have used the conventional Porto's notation $e_i(p_i,p_s)e_s$, where e_i and e_s are propagation directions of incoming and scattered photon, respectively, and p_i and p_s are directions of polarizer and analyzer for incoming and scattered photons, respectively.

[15] A. Mlayah, R. Carles, G. Landa, E. Bedel, and A. Muñoz-Yagüe, J. Appl. Phys. **69**, 4064 (1991).

[16] A. Pinczuk, A. A. Ballman, R. E. Nahory, M. A. Pollack, and J. M. Worlock, J. Vac. Sci. Technol. **16**, 1168 (1979).

[17] J. S. Blakemore, J. Appl. Phys. **53**, R123 (1982).

[18] L. A. Borisova, A. F. Kravcenko, K. N. Kot, and E. M. Skok, Fiz. Tekh. Poluprovodn. **6**, 799 (1972) [Sov. Phys. Semicond. **6**, 693 (1972)].

[19] D. E. Aspnes and A. A. Studna, Phys. Rev. B **27**, 985 (1983).